Photon-counting passive 3D image sensing and processing for automatic target recognition

Seokwon Yeom, Bahram Javidi [a], and Edward Watson [b]

School of Computer and Communication Engineering, Daegu University, Gyeongsan, Gyeongbuk, Republic of Korea 712-714;

[a]Dept. of Electrical and Computer Engineering, U-2157, University of Connecticut, Storrs, CT USA 06269-2157;

[b]U.S. Airforce Research Laboratory, Wright Patternson Air Force Base, OH USA 45433

ABSTRACT

In this paper we overview the nonlinear matched filtering for photon counting recognition with 3D passive sensing. The first and second order statistical properties of the nonlinear matched filtering can improve the recognition performance compared to the linear matched filtering. Automatic target reconstruction and recognition are addressed for partially occluded objects. The recognition performance is shown to be improved significantly in the reconstruction space. The discrimination capability is analyzed in terms of Fisher ratio (FR) and receiver operating characteristic (ROC) curves.

Keywords: Image recognition, Image reconstruction, Nonlinear matched-filtering, Integral imaging, Photon counting, Low light level, Three-dimensional image processing, Three-dimensional image acquisition.

1. INTRODUCTION

Automatic target recognition (ATR) with a photon counting detector has been researched in [1, 2]. Recently, nonlinear matched filtering and photon counting linear discriminant analysis have been proposed in [3] and [4], respectively. Photon counting recognition with computational integral imaging has been proposed for the partially occluded objects [5]. In this overview paper, we present the pattern recognition system based on Ref. 3 and Ref. 5. The robustness of the nonlinear matched filtering is in that the mean of the filtered output is constant varying the number of photons and the variance is proportional to the inverse of the average photon counts. For occluded objects, photon counting recognition system measures nonlinear correlation between reconstructed scenes of a reference target and estimated photon-counting scenes of unknown objects in 3D space. We reconstruct sectional images at arbitrary depths using computational integral imaging (II) method. The Poisson parameters of the photon counts on the reconstruction plane are estimated by maximum likelihood estimation (MLE). The first and second order statistical properties of the nonlinear matched filtering in 3D space are the same with the ordinary nonlinear matched filtering which is performed on the image plane. The performance of the recognition system is evaluated in terms of Fisher ratios and ROC curves.

The organization of the paper is as follows. In Section 2, we provide the reconstruction methods for irradiance scenes and photon counting scenes. The photon counting nonlinear matched filtering is reviewed in Section 3. Photon counting images are simulated from captured irradiance scenes. In Section 4, these simulated images are used to compute the performances of the nonlinear matched filtering. Summary follows in Section 5.

2. COMPUTATIONAL RECONSTRUCTION OF INTEGRAL IMAGING

In this paper, II recording system is composed of a micro-lens array, an imaging lens, and a CCD (charge-coupled device) array camera [3-6]. A number of small convex lenses in the lens array capture elemental images where the captured ray information appears as a two-dimensional (2D) image with different perspectives. In the computational reconstruction of II, each elemental image is projected through a corresponding virtual pinhole to the reconstruction plane with arbitrary depths [6]. The recognition of occluded objects has been researched using integral imaging in [7].
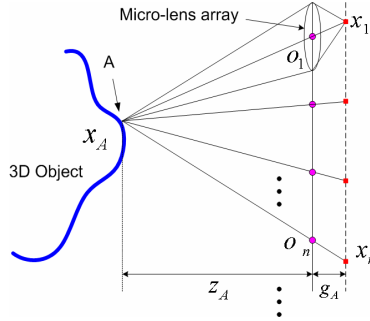
Fig. 1. II computational reconstruction model

Suppose that a point A in Fig. 1 is located at $[i_A, j_A, z_A]$ on the 3D object surface. The power density at the point A is denoted as x_A. Let x_n be the captured irradiance corresponding to the point A on the imaging plane of the n-th micro-lens. The points are located at $[i_n, j_n, g_A]$, $n=1,\ldots,N_A$ and assumed to have a unit area, o_n is the center of the n-th micro-lens. Under the assumption that the distance z_A between the point A and the micro-lens array is large enough, the same power is transferred from x_A and collected as $x_1,\ldots,x_{N_A}$, thus, the scale factors between x_A and x_n, $n=1,\ldots,N_A$ are approximately the same. Therefore, x_A can be estimated to be the average of x_n with a unit scale factor:

$$\hat{x}_A = \frac{1}{N_A}\sum_{n=1}^{N_A} x_n. \tag{1}$$

When the fluctuations in irradiance are assumed to be small compared to the fluctuations produced by the quantized nature of the radiation, we consider the Poisson distribution for the photon counting model [8]. The Poisson parameter for the photon-counts is assumed to be proportional to the irradiance on the detector. Therefore, the probability of photon count at pixel i is given by

$$P_d(y(i); \lambda(i)) = \frac{\lambda(i)^{y(i)} e^{-\lambda(i)}}{y(i)!}, \quad y(i) = 0,1,2,\ldots, \tag{2}$$

and

$$\lambda(i) = N_P[x(i)/\sum_{i=1}^{N_T} x(i)], \tag{3}$$

where $y(i)$ is the number of photons detected at pixel i, N_P is an expected number of photon-counts in the scene, $x(i)$ is irradiance at pixel i, N_T is the total number of pixels in the scene. Let y_n, $n=1,\ldots,N_A$ be the photon counts detected with the parameter λ_n which is associated with x_n. Let us consider λ_A which is associated with x_A. With the assumption that $x_1,\ldots,x_{N_A}$ are measurements of x_A, $\lambda_1,\ldots,\lambda_{N_A}$ are also originated from λ_n. Therefore, the joint probability density function of photon counts is calculated as

$$P_d(y_1,\ldots,y_{N_A}; \lambda_A) = \prod_{n=1}^{N_A} \frac{\lambda_A^{y_n} e^{-\lambda_A}}{y_n!}. \tag{4}$$

Thus, λ_A is estimated by the MLE (maximum likelihood estimation) [9] as

$$\hat{\lambda}_A = \frac{1}{N_A}\sum_{n=1}^{N_A} y_n. \tag{5}$$

3. NONLINEAR MATCHED FILTERING FOR PHOTON COUNTING RECOGNITION

For the recognition of photon counting scenes, the nonlinear matched filtering has been proposed as the nonlinear correlation normalized with the power v of the photon-counting image [3]:

$$C_{rs}(v) = \sum_{i=1}^{N_T} x_r(i) y_s(i) \left/ \left(\sum_{i=1}^{N_T} x_r(i)^2 \right)^{\frac{1}{2}} \left(\sum_{i=1}^{N_T} y_s(i) \right)^v \right. , \tag{6}$$

where $x_r(i)$ is the irradiance at pixel i of the reference target r, and $y_s(i)$ is the photon counts at pixel i of the unknown object s. The first and second order statistical properties of Eq. (6) is that the mean of $C_{rs}(1)$ is constant and the variance is approximately proportional to $1/N_P$ [3].

The nonlinear matched filtering in the reconstruction space has been proposed as follows [5]

$$D_{rs}(v) = \sum_{d=1}^{N_d} \left[\sum_{i \in \Omega_d} \hat{x}_r(i; z_d) \hat{\lambda}_s(i; z_d) \left/ \left(\sum_{i \in \Omega_d} \hat{x}_r(i; z_d)^2 \right)^{\frac{1}{2}} \left(\sum_{i \in \Omega_d} \hat{\lambda}_s(i; z_d) \right)^v \right. \right] , \tag{7}$$

where $\hat{x}_r(i; z_d)$ is the reconstructed irradiance information of the reference target at the depth z_d [See Eq. (1)], i denotes a virtual voxel on the reconstruction plane Ω_d, thus, voxels on the plane Ω_d have the same longitudinal distance z_d from the micro-lens array, $\hat{\lambda}_s(i; z_d)$ is the estimated Poisson parameter on the reconstruction plane Ω_d for the unknown input target [See Eq. (5)]. Since we have no prior information of the object location, the entire reconstruction space Ω_d, $d=1,\ldots,N_d$, is considered where N_d is the total number of depth levels which possibly cover the unknown object. The nonlinearity decided by v in the denominator in Eq. (7) have the same first and second order statistical properties with those of Eq. (6) since $\hat{x}_r(i)$ and $\hat{\lambda}_s(i)$ are the linear combination of the irradiance and the photon counts in the elemental images.

4. EXPERIMENTAL AND SIMULATION RESULTS

In this section, we present the experimental and simulation results of the photon counting recognition using nonlinear matched filtering on the image plane and in the reconstruction space.

4.1. Nonlinear matched filtering on the image plane

A micro-lens array and a pick-up camera are used to record elemental images. The pitch of each micro-lens is 1.09 *mm*, and the focal length of each micro-lens is about 3 *mm*. Three sets of elemental images have been obtained from three toy cars [3]. The size of each car is about 4.5 *cm* × 2.5 *cm* × 2.5 *cm*. The size of one elemental image array is 1600×1334 pixels. We simulate 1000 photon-limited images, each with a random number of photons following the Poisson distribution. Figure 2(a) shows the reference target and figures 2(b) and 2(c) are the false-class targets.
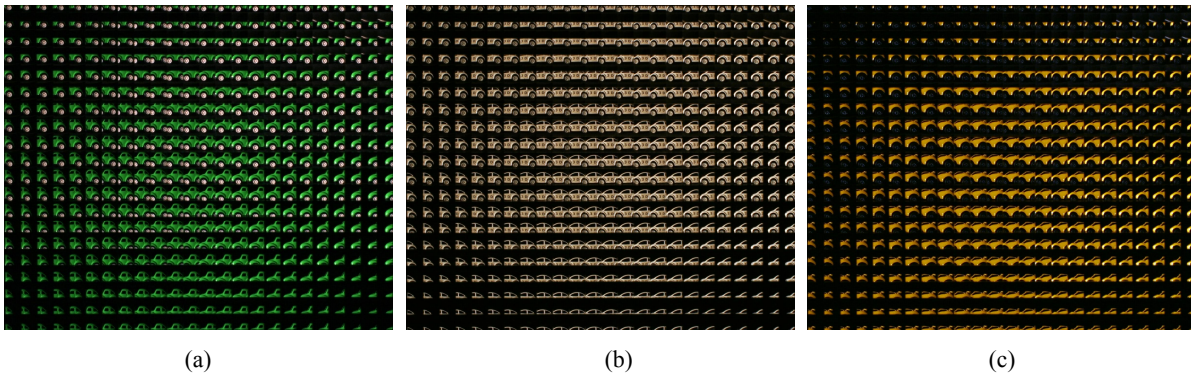

(a) (b) (c)

Fig. 2. Elemental images for (a) a reference target, car 1, (b) a false class target, car 2, (c) a false-class target, car 3.

Figure 3(a) shows the sample mean of correlation coefficients and the sample standard deviation when $v=1$ with theoretical prediction [3]. The red solid line graph represents the sample mean of autocorrelation between the irradiance image and photon counting images of car 1, and the blue dotted line and black dashed line graphs are the sample mean of cross-correlation between the irradiance image of car 1 and photon counting images of car 2 or car 3, respectively. Error

bars stand for $m_{rs} \pm \sigma_{rs}$ where m_{rs} and σ_{rs} are the sample mean and the sample standard deviation of the nonlinear matched filtering, respectively. Figure 3(b) shows the sample variance of $C_{rs}(0;1)$ with theoretical prediction [3]. The deviation from the theoretical prediction becomes larger as the number of photons decreases as shown in figure 3(b).
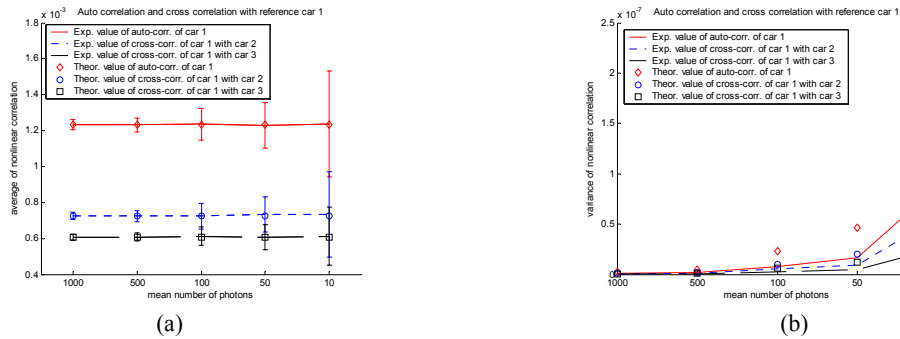

(a)   (b)

Fig. 3. Mean and variance of $C_{rs}(0;1)$, (a) sample mean and theoretical prediction, (b) sample variance and theoretical prediction.

Figures 4(a)-(d) show ROC curves corresponding to cars (r=1, s=2) and cars (r=1, s=3) for $C_{rs}(0;0)$ and $C_{rs}(0;1)$, respectively. Figures 4(b) and (d) show better performance than figures 4(a) and (c).

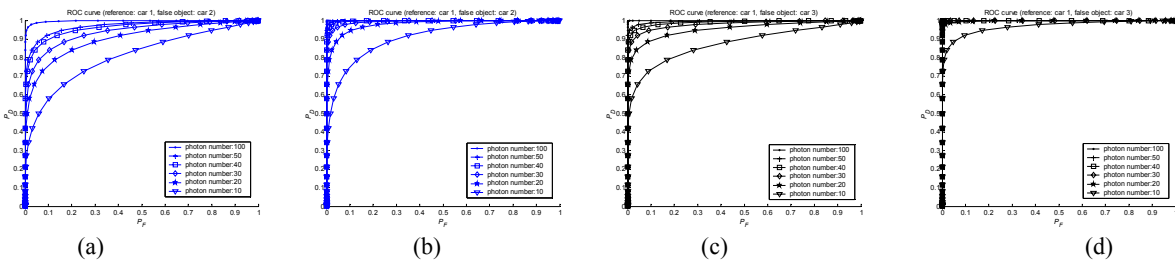(a)   (b)   (c)   (d)

Fig. 4. ROC curves when $r = 1$, (a) $s = 2$ for $C_{rs}(0;0)$, (b) $s = 2$ for $C_{rs}(0;1)$, (c) $s = 3$ for $C_{rs}(0;0)$, (d) $s = 3$ for $C_{rs}(0;1)$.

4.2. Nonlinear matched filtering in the reconstruction space

To simulate the partial occlusion, a tree model is placed between the toy car and the micro-lens array. Figure 5 shows the elemental images of the reference target, car 2 in this experiment and the partially occluded reference target and the false-class target, car 3 without occlusion. The size of one elemental image array is 1419×1161 pixels. Figure 6 show that the reconstructed sectional images in the 3D space for the partially occluded true-class target [See Fig. 5(b)].

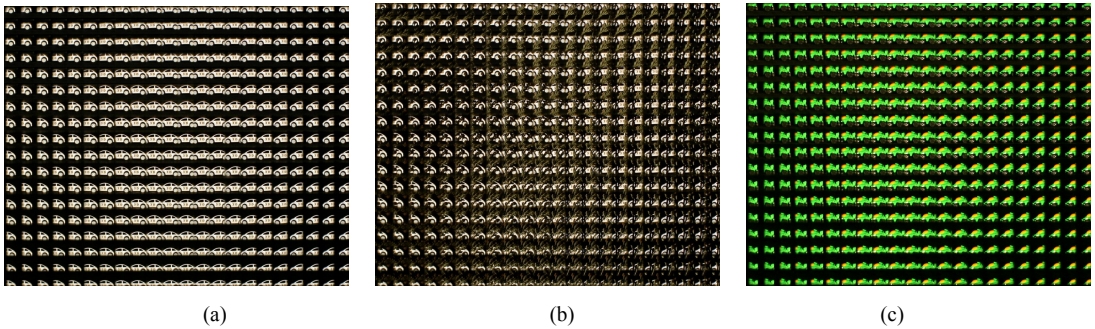(a)   (b)   (c)

Fig. 5. Elemental images for (a) the reference target, car 2 (b) the reference target, car 2 with partial occlusion, (c) the false-class target, car 3.

(a)   (b)

Fig. 6. Reconstructed images of the partially occluded true-class target, (a) d = 40 mm, (b) d = 74 mm.

One hundred photon counting images for each elemental image are generated to compute the means and variances of the nonlinear matched filtering. Figures 7(a) and 7(b) show the experimental results of nonlinear matched filtering for elemental images, that is without reconstruction [See Eq. (6)] and with reconstruction [See Eq. (7)], respectively. The red solid line graph represents the sample mean for the true class target with occlusion and the blue dotted line graph is the sample mean for the false class target. N_d in Eq. (7) is set at 1 where the depth of reconstruction plane is 74 mm. Figure 8(a) shows the Fisher ratios. Fisher ratio decreases when a lower number of photo-counts is used. Figures 8(b) and 8(c) show the ROC curves when N_p=500 and N_p=100, respectively. It is shown that the recognition performance of the proposed technique is substantially improved compared to the nonlinear matched filtering without reconstruction.

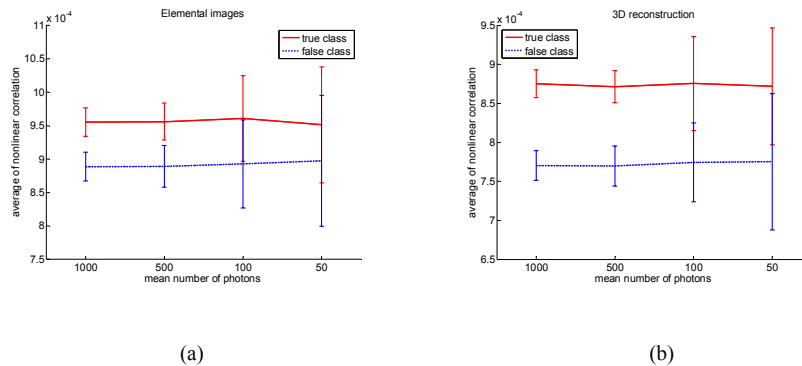(a)   (b)

Fig. 7. Sample mean and error bars (standard deviation) for nonlinear matched filtering using (a) elemental images without reconstruction, (b) reconstructed scenes in 3D space.
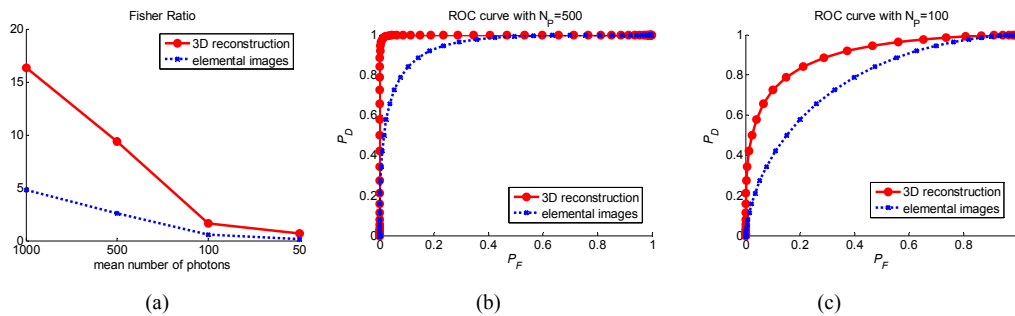

(a)   (b)   (c)

Fig. 8. Comparison of recognition performance between elemental images and 3D reconstruction, (a) Fisher ratios, ROC curves when (b) N_p=500, (c) N_p=100.

5. SUMMARY

In this paper we overview the nonlinear matched filtering on the image plane and in the reconstruction space. The first and second order statistical properties of the nonlinear matched filtering are shown to provide better recognition

performance than the linear matched filter in terms of Fisher ratio and ROC curves. The computational II visualizes the occluded object by reconstructing sectional images in 3D space. Photon counting scenes are estimated using MLE of the Poisson parameters in 3D space. We have shown that the output of the nonlinear matched filtering in 3D space provides improved performance than the nonlinear matched filtering on the image plane for the partially occluded objects.

Acknowledgements

REFERENCES

[1] Morris, G. M., "Scene matching using photon-limited images," J. Opt. Soc. Am. A. 1(5), 482-488 (1984).
[2] Watson, E. and Morris, G. M., "Comparison of infrared upconversion methods for photon-limited imaging," J. Appl. Phys. 67(10), 6075-6084 (1990).
[3] Yeom, S., Javidi, B., and Watson, E., "Photon counting passive 3D image sensing for automatic target recognition," Opt. Express 13(23), 9310-9330 (2005).
[4] Yeom, S., Javidi, B., and Watson, E., "Three-dimensional distortion-tolerant object recognition using photon-counting integral imaging," Opt. Express 15(4), 1513-1533 (2007).
[5] Yeom, S., Javidi, B., Lee, C. W., and Watson, E., "Photon-counting passive 3D image sensing for reconstruction and recognition of partially occluded objects," Opt. Express 15(24), 16189-16195 (2007).
[6] Hong, S. H., Jang, J. S., and Javidi, B., "Three-dimensional volumetric object reconstruction using computational integral imaging," Opt. Express 12(3), 483-491 (2004).
[7] Javidi, B., Ponce-Diaz, R., and Hong, S. H., "Three-dimensional recognition of occluded objects by using computational integral imaging," Opt. Letter 31(8), 1106-1108 (2006).
[8] Goodman, J. W., [Statistical Optics], Jonh Wiley & Sons, inc., (1985).
[9] Kay, M., [Fundamentals of Statistical Signal Processing], Prentice Hall, New Jersey, (1993).